Research

The maturational characteristics of the GABA input in the anterior piriform cortex may also contribute to the rapid learning of the maternal odor during the sensitive period

Enver Miguel Oruro,[1,2,3,7] Grace V.E. Pardo,[3,4,5,6,7] Aldo Bolten Lucion,[2,4] Maria Elisa Calcagnotto,[2,3] and Marco A.P. Idiart[1,2]

[1]*Neurocomputational and Language Processing Laboratory, Institute of Physics, Universidade Federal do Rio Grande do Sul, Porto Alegre, Rio Grande do Sul 91501-970, Brazil;* [2]*Neuroscience Graduate Program, Universidade Federal do Rio Grande do Sul, Porto Alegre, Rio Grande do Sul 90050-170, Brazil;* [3]*Neurophysiology and Neurochemistry of Neuronal Excitability and Synaptic Plasticity Laboratory, Department of Biochemistry, Instituto de Ciências Básicas da Saúde (ICBS), Universidade Federal do Rio Grande do Sul, Porto Alegre, Rio Grande do Sul 90035-003, Brazil;* [4]*Department of Physiology, ICBS, Universidade Federal do Rio Grande do Sul, Porto Alegre, Rio Grande do Sul 90050-170, Brazil;* [5]*Centre for Interdisciplinary Science and Society Studies, Universidad de Ciencias y Humanidades, Los Olivos, Lima 15314, Peru;* [6]*Center for Biomedical Research, Universidad Andina del Cusco, San Jerónimo, Cuzco 08006, Peru*

During the first ten postnatal days (P), infant rodents can learn olfactory preferences for novel odors if they are paired with thermo-tactile stimuli that mimic components of maternal care. After P10, the thermo-tactile pairing becomes ineffective for conditioning. The current explanation for this change in associative learning is the alteration in the norepinephrine (NE) inputs from the locus coeruleus (LC) to the olfactory bulb (OB) and the anterior piriform cortex (aPC). By combining patch-clamp electrophysiology and computational simulations, we showed in a recent work that a transitory high responsiveness of the OB-aPC circuit to the maternal odor is an alternative mechanism that could also explain early olfactory preference learning and its cessation after P10. That result relied solely on the maturational properties of the aPC pyramidal cells. However, the GABAergic system undergoes important changes during the same period. To address the importance of the maturation of the GABAergic system for early olfactory learning, we incorporated data from the GABA inputs, obtained from in vitro patch-clamp experiment in the aPC of rat pups aged P5–P7 reported here, to the model proposed in our previous publication. In the younger than P10 OB-aPC circuit with GABA synaptic input, the number of responsive aPC pyramidal cells to the conditioned maternal odor was amplified in 30% compared to the circuit without GABAergic input. When compared with the circuit with other younger than P10 OB-aPC circuit with adult GABAergic input profile, this amplification was 88%. Together, our results suggest that during the olfactory preference learning in younger than P10, the GABAergic synaptic input presumably acts by depolarizing the aPC pyramidal neurons in such a way that it leads to the amplification of the pyramidal neurons response to the conditioned maternal odor. Furthermore, our results suggest that during this developmental period, the aPC pyramidal cells themselves seem to resolve the apparent lack of GABAergic synaptic inhibition by a strong firing adaptation in response to increased depolarizing inputs.

[Supplemental material is available for this article.]

Infants of altricial animals learn very rapidly to attach to their mothers. While essential for the immediate survival, these early experiences may also have long lasting consequences in adulthood. Understanding the mechanisms involved in the developing neural circuits underlying this first affiliative behavior is a critical step toward understanding the impact of the mother's care on the behavioral outcomes of the adult offspring, including mental health issues in the case of humans (Perry et al. 2017; Sullivan and Opendak 2018).

Newborn rodents are blind, deaf and possess limited motor skills. They are confined to the nest for the first 2 wk of postnatal life. Recognizing the mother's odor during this period is crucial for odor-guided behaviors such approaching the mother and attaching to a nipple (Farrell and Alberts 2002; Moriceau and Sullivan 2004; Kojima and Alberts 2009; Raineki et al. 2010; Meyer and Alberts 2016; Al Aïn et al. 2017). It is presumed that the pups learn the mother's odor by associating it with maternal care during the first 10 postnatal days (Moriceau and Sullivan 2005). This hypothesis has been extensively tested in an experimental paradigm where young rodents were subjected to pairings of an artificial odor (the unconditioned stimulus) with tactile stimulation, such as brush strokes, to mimic the presence of the mother

[7]**These authors contributed equally to this work.**
Corresponding author: envermiguel@gmail.com
Article is online at http://www.learnmem.org/cgi/doi/10.1101/lm.052217.120.

(the conditioned stimulus). Results shows that animals younger than P10 display orientation approximation behavior toward the artificial odor (Moriceau and Sullivan 2005; Morrison et al. 2013; Roth et al. 2013; Ghosh et al. 2015). However, pairing becomes ineffective for older than P10 age (Moriceau and Sullivan 2005; Morrison et al. 2013; Roth et al. 2013; Ghosh et al. 2015), but learning can be reinstated by direct application of NE in the OB or LC stimulation, which may suggest that the learning changes could be due to local LC changes (Sullivan et al. 2000).

It has been proposed that the olfactory circuit primarily including the OB and the aPC, both modulated by NE inputs from LC, is sufficient to support this learning (Sullivan et al. 1991, 1992, 1994; Morrison et al. 2013; Ghosh et al. 2017). In fact, in vivo studies show that the LC of neonate rats have large responses to somatosensory stimuli (Kimura and Nakamura 1985) and high levels of NE are released in the OB during odor-stroke conditioning in pups younger than P10, but this is no longer observed in pups older than P10 (Rangel and Leon 1995). Although, for pups older than P10, the pairing of an odor with electrical stimulation of NE fibers projecting to the OB results in preference for that odor (Wilson and Sullivan 1992). Moreover, in the aPC, NE release seems to be necessary and sufficient for the early odor preference learning. The pairing of an artificial odor with pharmacological activation of β-adrenoceptors, in the absence of any tactile stimulation or direct LC activation, induce behavioral olfactory preference in pups younger than P10. On the other hand, the blockage of the β-adrenoceptors before the odor-stroke pairing prevents the acquisition of odor preference (Morrison et al. 2013; Ghosh et al. 2015, 2017). In addition to the NE release, an elevated plasticity at the OB-aPC sensory synapses is present for ages younger than P10 (Franks and Isaacson 2005; Poo and Isaacson 2007) what has been considered critical to early olfactory learning (Yuan et al. 2014). The blockage of excitatory synaptic plasticity in the aPC before odor-stroke pairing, by blocking NMDA receptors, prevent the preference learning in pups younger than P10 (Morrison et al. 2013; Mukherjee and Yuan 2016; Ghosh et al. 2017).

In recent work, we proposed an alternative explanation based on a computational model of the OB-aPC circuit (Fig. 1) where we added aPC pyramidal cells age-dependent intrinsic properties obtained in our laboratory by in vitro patch-clamp electrophysiology of aPC slices from P5–P8 and P14–P17 infant rats (Oruro et al. 2020). We used the model to simulate a classical conditioning paradigm by pairing an odor (a random input to the network representing the maternal odor) with NE release (changes in neuronal properties, representing the maternal care) and then after the pairing protocol we measured the activity of the aPC pyramidal cells in response to the maternal odor exposition. We found that the OB-aPC circuit shows a higher aPC pyramidal activation to the maternal odor at ages P5–P8 than at ages P14–P17, and this can be explained by the changes in the intrinsic properties of the pyramidal cells due to maturation, indicated by our electrophysiological data. We also propose that, similarly, the experiments using artificial odors could be explained by an overlap between the novel odor neural representation at aPC (after pairing it with strokes) and the mother's odor neural representation at aPC, and this effect is prominent at P5–P8 and occur to a lesser extent at P14–P17 (Oruro et al. 2020).

In this work, we add yet another ingredient to our model. In addition to the age-dependent changes of aPC pyramidal cells, another intrinsic developmental mechanism could contribute to facilitate the higher responsiveness of pyramidal cells for the maternal odor at P5–P8. Previous study has shown that activation of $GABA_A$ receptor by local infusion of agonist prevents the olfactory conditioning learning in rat pups younger than P10 (Morrison et al. 2013). Recent experimental work had shown that the GABAergic inputs to the aPC pyramidal cells at the P5–P8 age are reduced compared to older ages (Pardo et al. 2018). In addition, we found in the present study that the $GABA_A$ receptor equilibrium potential (E_{GABA}) is more depolarized than the resting membrane potential and the threshold of the aPC pyramidal cells recorded in pups from the same age period. To address the impact of this developmental change to the maternal odor learning, we include a variable GABAergic synaptic input to our previous P5–P8 OB-aPC circuit model and simulate the maternal odor learning by pairing odor input with norepinephrine (NE) release. Simulations revealed that OB-aPC circuits modeled with GABAergic synaptic inputs present an even more significant number of active cells in response to the maternal odor, suggesting that during this period of development, the GABAergic synapses also contribute to support higher responsiveness to the maternal odor.

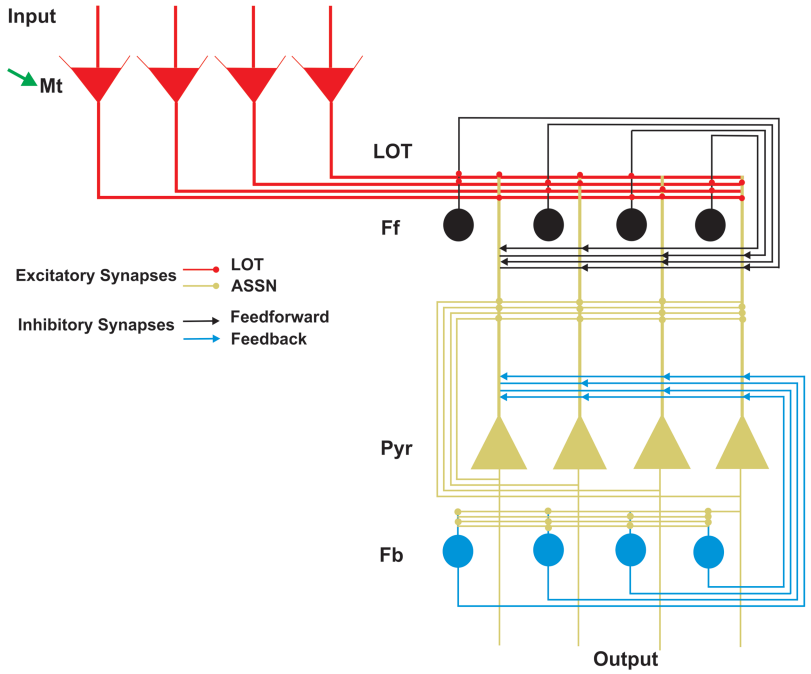

Figure 1. A simplified architecture of the artificial circuit of the olfactory system. The figure is a simplified structure of the olfactory bulb (OB), containing only the mitral cells (Mt; red), and the anterior piriform cortex (aPC) with principal kinds of cells: pyramidal cells (Pyr; yellow), feed-forward (Ff; black), and feedback (Fb; blue) interneurons. The axons of the Mt cells extend to the aPC forming the lateral olfactory tract (LOT; red). The LOT terminals make excitatory synapses (red dots) with the apical dendrites of the Pyr cells and with the Ff interneurons. In turn, the Ff interneurons make inhibitory synapses on the dendrites of Pyr cells (black arrows). The Pyr cells form an important associative input making excitatory synapses with another adjacent Pyr cells and with Fb interneurons (ASSN; yellow dots). In turn, Fb interneurons make inhibitory synapses with basal dendrites and soma of Pyr cells (blue arrows). Mt cells are modulated by NE (green arrow).

Results

Computational experiment 1: GABAergic synaptic input enhances the learning of the maternal odor

The maturational characteristics of the GABAergic synaptic input in the aPC during the P5–P8 age period (the sensitive period for attachment learning) contributes to the maternal odor learning. Specifically, simulation results of classical conditioning of two P5–P8 OB-aPC circuits (Fig. 2A) revealed that circuits modeled with GABAergic input profile (see Table 1) increased their activity in response to the conditioned maternal odor. Figure 3 shows the activity profiles of the aPC before, during, and after conditioning in two situations with the introduction of GABA synapses and without the introduction of GABAergic synapses. Before conditioning, the P5–P8 OB-aPC circuit "with GABA" exhibited a slightly higher response to odor when compared to the circuit "without GABA." Over the seven sessions of odor-NE pairing, the activity of the circuit "with GABA" was twice higher than the circuit "without GABA" (Fig. 3B,C; red dots). At the last trial session, the number of spikes and the number of active cells reached their maximum increase of 179% and 134%, respectively (taking the maximal number of evoked spikes during the first trial as 100%, from 10 respiratory cycles).

After conditioning, the average maximum number of spikes (86 ± 2.07 vs. 46.50 ± 0.88) (Fig. 3B, inserted graph) and the average maximum number of active cells (83.16 ± 1.88 vs. 44.13 ± 0.13) (Fig. 3C, inserted graph) were higher when GABA was present [number of spikes: $t_{(14)} = 17.53$; number of active cells: $t_{(14)} = 20.75$; both $P < 0.0001$, unpaired t Student test]. These results indicate that both circuits, with and without GABAergic synaptic inputs, learn the maternal odor; however, in the presence of GABA inputs the pyramidal cells exhibit an enhanced response for the conditioned maternal odor. It could be the that the GABAergic contribution is restricted only to the training phase, by allowing a higher recruitment of pyramidal cells during odor pairing with NE, but with little effect afterward. To clarify that, in the next section we measured the effect of GABA during recall.

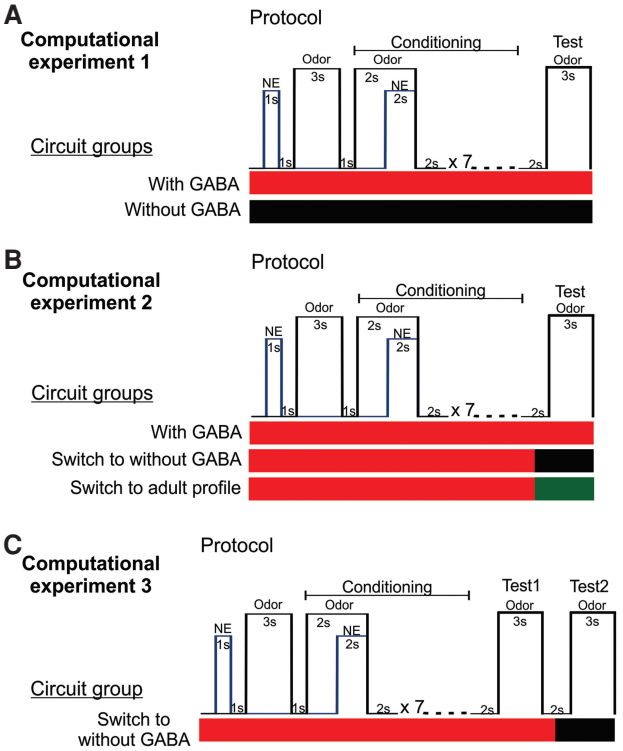

Figure 2. Computational experimental design and conditioning protocols. (*A*) Computational experiment 1. Two OB-aPC circuits groups, modeled with GABA (red horizontal bar) and without GABA (black horizontal bar) were separately conditioned using a delayed pairing procedure of odor and NE. In the protocol, the odor onset preceded the NE onset by 2 sec, odor-NE overlapping for 2 sec, after which the odor was terminated. This pairing was presented seven times with a 2-sec interval. Two seconds after the last pairing, the odor was presented alone during a 3-sec window. (*B*) Computational experiment 2. OB-aPC circuits modeled with GABA were conditioned (red horizontal bar) using the same previous protocol, and 1 sec after the last pairing, the GABAergic synaptic input was blocked (black horizontal bar), or switched to adult GABAergic input profile (green horizontal bar) and the recall (test) was measure in those conditions. (*C*) Computational experiment 3. OB-aPC circuits modeled with GABA (red horizontal bar) using the same odor-NE pairing protocol and 2 sec after the last pairing were tested for the recall 1 of the maternal odor (test 1). One second after the recall 1 was finished, the GABAergic input was blocked (black horizontal bar) and the plasticity of mitral cell and pyramidal cells was excluded. In those conditions, the activity of the circuits was measured during another 3 sec window to the recall 2 of the maternal odor (test 2).

Computational experiment 2: GABAergic synaptic input amplifies the recall of the maternal odor

In order to test the individual effect of GABA in recall, three groups of P5–P8 OB-aPC circuits "with GABA" were trained (Fig. 2B) and after the last pairing, three different recall conditions where explored (Fig. 4A): The GABA input properties remained the same ("with GABA"), were blocked ("without GABA"), or switched to adult GABAergic input profile ("with adult profile"). The aPC pyramidal cells activity in the "without GABA" ($n = 10$ circuits) (Fig. 4B, C; black dots) or "with adult profile" conditions ($n = 10$ circuits) (Fig. 4B,C; green dots) show a significant reduction in the number of spikes (one-way ANOVA, $F_{(2,21)} = 598.1$; $P < 0.0001$, followed by Tukey test; $n = 8$ respiratory cycles in each condition) when compared with the "with GABA" condition ($n = 10$ circuits). The same is true for the number of active cells (one-way ANOVA, $F_{(2,21)} = 597$; $P < 0.0001$, followed by Tukey test; $n = 8$ respiratory cycles in each condition) (Fig. 4B,C; red dots). Moreover, the circuit "with adult profile" has a dramatic reduction in the maximum number of spikes and a number of active cells when compared to the two other conditions (Fig. 4B,C, inserted graphs). These results indicate that the GABAergic input per se contributes to the amplified response during the recall of the maternal odor. Next, we investigated whether the individual variability of the circuits in the experimental groups (intersubject design) (see Fig. 2B), which was modeled by randomizing the connectivity, may have partly contributed to this result.

Computational experiment 3: GABAergic synaptic input amplifies the recall of the maternal odor independently of the variability of the circuit

To control possible effects of the variability of connections between the models, a group of P5–P8 OB-aPC circuits, modeled "with GABA" input ($n = 10$ circuits), was submitted to the conditioning protocol (Fig. 2C) where two recall phases 2 sec apart were tested. We found that all pyramidal cells that fired during the recall 1 phase reduced their spiking frequency significantly in the recall 2 phase (Fig. 5B shows a representative spiking profile from an aleatory aPC pyramidal cell). The mean of the number of spikes (recall 1: 94.69 ± 0.76, $n = 8$ respiratory cycles vs. recall 2: 76.23 ± 0.45, $n = 7$ respiratory cycles; $t_{(6)} = 15.57$; $P < 0.0001$; paired t Student test) (Fig. 5C, inserted graph) and the mean of the number of active cells (recall 1: 83.49 ± 0.52, $n = 8$ respiratory cycles vs. recall 2: 71.67 ± 0.35; $n = 7$ respiratory cycles; $t_{(6)} = 20.35$; $P <$

Table 1. Model parameters

Neurons	Parameters
Mitral (Mt) cells ($n = 100$ cells)	$\tau = 20$ ms $\Theta_{min} = -0.0014$ V; $\Theta_{max} = 0.009$ V[a] $\Theta_{min} = -0.0014$ V; $\Theta_{max} = 0.002$ V[b] $V_{hyper} = -0.01$ V; $t^{refrac} = 2$ msec
Pyramidal (Pyr) cells ($n = 200$ cells)	$\Theta_{min} = -0.03922$ V; $\Theta_{max} = -0.03663$ V[c] $V^{hype} = \Theta_{min}$; $t^{refrac} = 2$ msec $\tau = 42.78$ msec[c] $C_m = 98.21$ pF[c] $R_{inp} = \tau/C_m$ MΩ[c] $AP_{ampl} = 0.07690$ V[c] $E_{ahc} = -0.060$ V[d] $\tau_{ahc} = 1$[d] $A_{ahc} = 30$[d] $Rm_{adapt} = 0.12$[e] $W_{Mt\ to\ Pyr} = 35$[e] $g^{max}{}_{Pyr\ to\ Pyr} = 10$[e] $W_{Pyr\ to\ Pyr} = 35$[e] $g^{max}{}_{Mt\ to\ Pyr} = 10$[e] $E_{glu} = 0$ V $\tau_{2\ Mt\ to\ Pyr} = 1$ msec; $\tau_{2\ Mt\ to\ Pyr} = 2$ msec $\tau^{pp} = 12$ msec $\tau^{pnp} = \tau^{npp} = 500$ msec $W_{LTP} = 62.2$ $W_{LTD} = 12.25$ $E_{GABA} = -0.02458$ V[c] $\tau_{2\ Ff\ to\ Pyr} = 4.8$ msec; $\tau_{2\ Ff\ to\ Pyr} = 5.36$ msec[c] E_{GABA} adult $= -0.070$ V
Feed-forward (Ff) interneurons ($n =$ 100 cells)	$\tau = 15$ msec $\Theta_{min} = 0$ V; $\Theta_{max} = 0.015$ V $V^{hyper} = -0.01$ V $g^{max}{}_{Ff\ to\ Pyr} = 13693, 7096$[d] $E_{Glu} = 0$ V $\tau_{2\ Py\ toff} = 1$ msec; $\tau_{2\ Pyr\tau\ to\ ff} = 2$ msec[c]
Feedback interneurons (Fb) ($n = 100$ cells)	$\tau = 5$ msec $\Theta_{min} = 0$ V; $\Theta_{max} = 0.013$ V $V^{hyper} = -0.01$ V $g^{max}{}_{Fb\ to\ Pyr} = 13693, 7096$[d] $E_{Glu} = 0$ V $\tau_{2\ Pyr\ to\ Fb} = 1$ ms; $\tau_{2\ Pyr\tau\ to\ Fb} = 2$ msec

[a]Values without NE modulation.
[b]Values with NE modulation.
[c]Values from electrophysiological data.
[d]Values inferred from electrophysiological data reported in this study.
[e]Values inferred from electrophysiological data reported in the literature.

0.0001; paired *t* Student test) (Fig. 5D, inserted graph) were significantly reduced in the recall 2 phase when compared with recall 1. Moreover, we observed that onset of the pyramidal cell activity was closer to the rising phase of inhalation during recall 1, but was delayed to the middle of the inhalation phase during recall 2. This computational experiment (intrasubject design) (see Fig. 2C) confirms that the GABAergic input per se contributes to the amplification of the response of the P5–P8 OB-aPC circuit for the conditioned maternal odor.

Discussion

Previous studies of early olfactory learning in infant rodents (mostly rats and mice) have pointed the OB and aPC as crucial areas, in which NE release is both necessary and sufficient for infant olfactory learning (for a revision, see Moriceau and Sullivan 2005; Yuan et al. 2014). The main contributions of the present study are (1) to propose a model of the OB-aPC circuit for the maternal odor learning during the sensitive period based on the GABAergic synaptic input profile, in addition to the aPC experimental intrinsic electric properties of pyramidal cells, and (2) to reveal that the GABAergic synaptic input profile during this period also contributes to supporting the maternal odor learning and the recall process.

Does GABAergic input in aPC contributes to the maternal odor learning during the sensitive period?

In this work, we investigate the possible contribution of GABAergic synapses into our model for early olfactory learning. We found that adding GABAergic inputs increased by 47% both the number of active pyramidal cells in aPC and their spiking activity in response to the conditioned odor (Fig. 3). Moreover, we found that GABA is not only relevant during learning but also in the recall phase (Fig. 4). The contribution for immature GABA cells was able to increase in 70% the number of pyramidal cells in aPC that were responsive to the learned odor when compared to the scenario where these cells have the adult profile (Fig. 4). Finally, after eliminating any possible effect of random connections in the OB-aPC circuit on the effect of GABAergic input in the maternal odor recall, we tested the circuit for two recall scenarios (with intact or blocked GABA input) after odor conditioning. We found that blocking GABA input reduced the number of active cells (15%) and spiking activity (20%), suggesting that the GABAergic input in the aPC amplifies the ability of the circuit to support the recall process of the maternal odor (Fig. 5). Therefore, we showed that GABAergic input characteristic of P5–P7 contributes to the maternal odor learning and this contribution resides in the ability to amplify the response of the OB-aPC circuit to the conditioned maternal odor in terms of both numbers of active cells and spikes.

How does the GABAergic input in aPC manage to amplify the activity of pyramidal cells during the sensitive period?

We found that the E_{GABA} of the aPC pyramidal cells from P5–P8 animals was more depolarized (−24.58 mV) (reported in the present study) in comparison with the resting membrane potential and the voltage threshold potential of the same type of cells (−40.27 mV and −35.94 mV, reported in our previous work (see Fig. 6; Oruro et al. 2020). The E_{GABA} of the aPC pyramidal cells from P5–P8 animals was also ∼18 mV more depolarized than the value obtained in older pups (GVE Pardo, AB Lucion, ME Calcagnotto, et al. unpubl.). This result strongly suggests that during the sensitive period of attachment learning, the activation of GABA synapses produces depolarization in the aPC pyramidal cells instead of the characteristic hyperpolarization. It is not uncommon phenomena in developing cortices. Excitatory GABA has been reported for many immature brain areas attributed to the positive switch in the chloride reversal potential due to elevated intracellular chloride concentration (Rivera et al. 1999; Rheims et al. 2008; Ehrlich et al. 2013; Tyzio et al. 2014) and for revision see (Ben-Ari 2014)).

If GABAergic input to aPC pyramidal cells is excitatory during this period, as we are suggesting, why is that the local infusion of GABA receptor agonist (muscimol) into the aPC 10 min before odor-stroke training has shown to prevent the olfactory preference learning in P7 age rat pups?

A possible answer to this question arises from our experimental observation of the active membrane properties of the aPC pyramidal cells during this period of development. In the experiment by

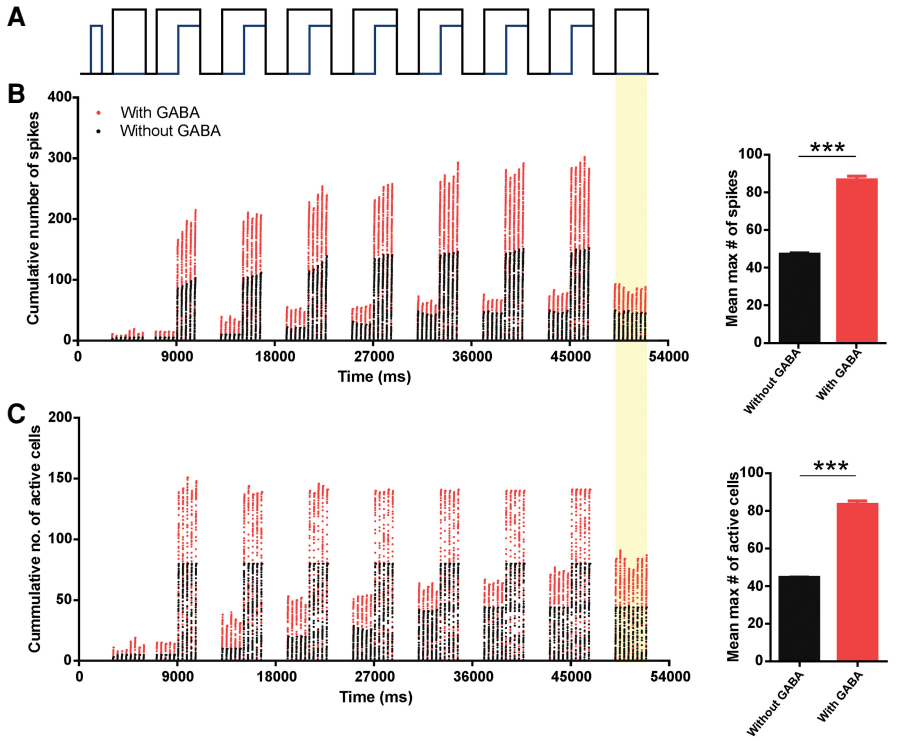

Figure 3. Cumulative number of spikes and number of active aPC pyramidal cells during maternal odor conditioning in the P5–P8 OB-aPC circuit with and without GABA synaptic input. (*A*) Protocol for odor conditioning. A delayed pairing procedure was used in which the odor (black trace) onset preceded the NE (blue trace) by 2 sec and odor and NE overlapped for 2 sec, after which the odor was terminated. The odor-NE pairing was presented seven times with 2 sec intervals. Plot of cumulative number of spikes (*B*) and number of active cells (*C*) during odor-NE pairing and odor test are showed for the P5–P8 OB-aPC circuit with GABA input (red dots) superimposed to the circuit without GABA input (black dots). Data were collected at every 0.5 msec in a 200-msec window of simulation. Simulation (from 0 msec to 54,000 msec) was carried out over several respiratory cycles modulating the activity of the mitral cells, starting with 200 msec of the exhalation phase followed by 200-msec inhalation phase. Activity was measured during inhalation and exhalation phase. After conditioning, the test of the odor (yellow background) evoked a higher cumulative number of spikes and number of active cells for the circuit with GABA input compared to the cells for the circuit without GABA input (inserted graphs). Asterisks represent statistically significant unpaired *t* Student test comparison between the groups during the odor test. (***) $P < 0.001$. Bin: 0.5 msec.

Morrison et al. (2013), the injection of muscimol into the aPC was used to increase the inhibitory synaptic effect of GABA onto the pyramidal cells. The effect of muscimol can be interpreted as a constant excitatory synaptic effect of GABA similar to the effect of the sustained depolarizing current into the pyramidal cells on in vitro current clamp experiment, as we have observed in our previous experiments (Oruro et al. 2020). The aPC pyramidal cells of P5–P8 pups exhibit adaptation properties to increasing depolarizing inputs but this is no longer observed in older pups (Supplemental Fig. S1). In Figure 7, pyramidal cells respond maintaining constant or reducing their firing to increasing inputs, which suggest that aPC pyramidal cells can eventually reduce or interrupt their activity in response to increasing GABAergic input. Thus, the local infusion of muscimol into the aPC may be equivalent to the synaptic activity of all GABAergic neurons at the same time, which in physiological conditions is unlikely to occur. Therefore, if the aPC pyramidal cells show adaptation, the resulting increase in depolarizing inputs could have inhibitory effect in their activity. This effect could be progressively reduced with development, as data from older pups seem to indicate, since E_{GABA} tends to change to more hyperpolarized values (GVE Pardo, AB Lucion, ME Calcagnotto, et al., unpubl.). This also suggests that the firing adaptation properties of the aPC pyramidal cells could be the way to manage the lack of synaptic inhibition in the circuit during early development period.

It is interesting to think that during the P5–P8 age period, the inhibition in the aPC is provided by the action potential properties of pyramidal cells itself and not by the GABA synaptic conductance. However, it remains to be verified if indeed the GABAergic synaptic transmission in the aPC during the sensitive period of attachment learning is excitatory, how the depolarizing GABA could influence the pyramidal cells' excitability and how it could amplify the response to the entrance of odor remains for future work. Interestingly, inhibitory action of GABA has been proposed to be critical for the emergence of aversive conditioned responses induced by odor-shock pairing. In P11 rodents, $GABA_B$ receptor activation prevents the acquisition of olfactory preference learning induced by pairing odor with electric shock, and its pharmacological blocking paired with an odor induce an aversive response to that odor (Okutani et al. 2003). $GABA_A$ receptor activation also has been reported to be critical for the long-term depression in excitatory synapsis in the basolateral amygdala, which correlates with the emergence of conditioned odor aversion in rodent pups older than P10 (Thompson et al. 2008). For an excellent revision in the matter see (Ross and Fletcher 2019).

In conclusion, our computational experiments show that the GABAergic input enhances the OB-aPC circuit's ability for maternal odor learning and amplifies its recall. Such effect is due to the maturational characteristics of the GABAergic inputs that depolarize aPC pyramidal neurons at age younger than P10. Furthermore, in this developing circuit, the apparent lack of synaptic inhibition mediated by GABA appears to be compensated by the adaptive firing properties of aPC immature pyramidal neurons. The depolarizing GABA input may contribute, at least in part, to induce the immature pyramidal neuron to reach its adaptive firing pattern therefore preventing runaway excitation in the circuit. The panorama unfolded here indicates that although an immature circuit may present very different properties regarding its individual cell types, this does not render the circuit useless. On the contrary, immature cells may provide the circuit with important computational properties while the stability of the circuit as a whole remains unchanged.

Materials and Methods

Circuit model and connectivity

The model presented here is an extension of our previous work (Oruro et al. 2020). The OB and aPC are implemented in separate subnetworks (de Almeida et al. 2013, 2016). Only the mitral cells (Mt) were implemented in the OB, which projects to the aPC by the lateral olfactory tract (LOT), as shown in Figure 1. The aPC was implemented with three cell types: pyramidal (Pyr) cells, feedforward (Ff) interneurons, and feedback (Fb) interneurons (Stokes

and Isaacson 2010; Bekkers and Suzuki 2013), with parameters listed in Table 1.

The present model contains 100 neurons of Mt cells, 200 neurons of Pyr cells, and 100 neurons of each type of interneurons (Ff and Fb). In our previous work, we adjusted the parameters for connectivity of Mt and Pyr cells to best match the experimentally reported data (Oruro et al. 2020). We assume that each Pyr cell is randomly connected with ~15–45 Mt cells. For the autoassociative Pyr–Pyr connectivity, we considered that each Pyr cell is randomly connected with five to 15 Pyr cells. This model does not consider the feedback interaction between the aPC and OB. The Ff interneurons receive excitatory input from Mt cells via the lateral olfactory tract (LOT) and connect the distal apical dendrites of the L2/3 Pyr cells (Suzuki and Bekkers 2007; Bekkers and Suzuki 2013). In our model, each Pyr cell is connected to 40% of the Ff interneurons population. Each Fb cell is excited by 25% random Pyr cells, and each Pyr cell is connected to 40% of the Fb cells. The parameters for the connectivity of Ff and Fb interneurons were adjusted using experimental data reported in our previous work (Pardo et al. 2018) and with data reported here (Table 2). To assure continuity between models, the architecture and parameters in the model, other than those related to the function of GABAergic input investigated here, were kept the same as the previous model (Oruro et al. 2020), as detailed in Table 2. Details about connectivity can be found in Figure 1, and all neural and synaptic parameters are detailed in Table 1.

The computational model and simulations were developed using NetLogo 6.0.4 software (NetLogo, http://ccl.northwestern.edu/netlogo, June 4, 2018). In the framework of NetLogo, each neuron was represented as an individual agent that processes information.

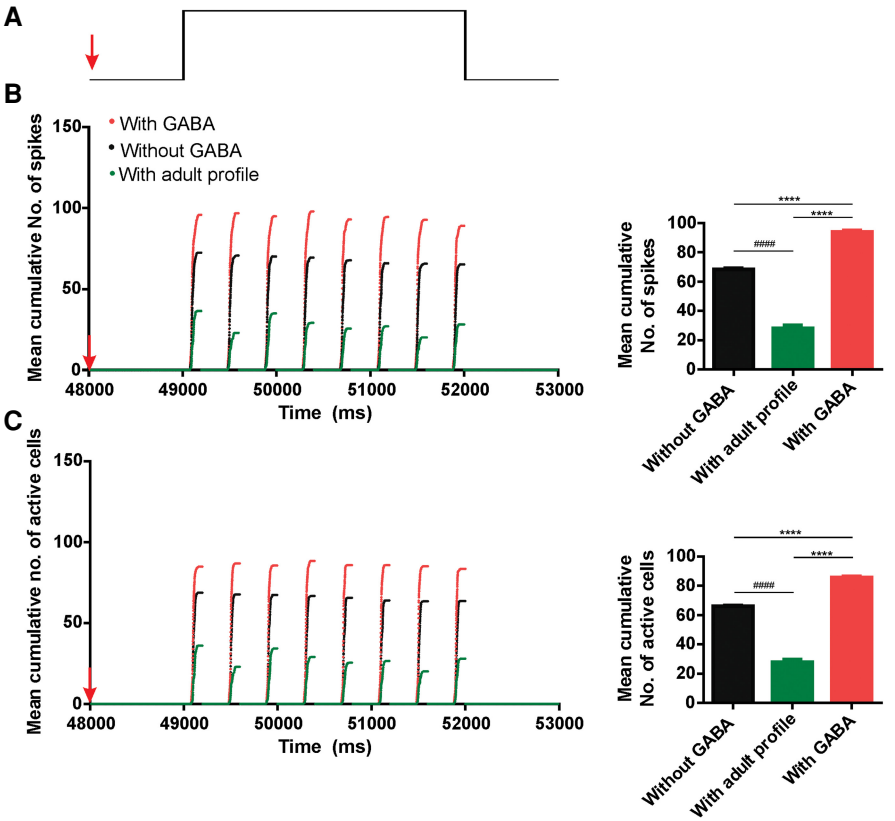

Figure 4. Comparative cumulative number of spikes and active number of cells during maternal odor recall in the P5–P8 OB-aPC circuit with GABA, without GABA and adult GABAergic input profile. (*A*) Illustration of the protocol of recall of CS (during 3 sec), which onset 2 sec after the last odor-NE pairing. Superimposed plot of cumulative number of spikes (*B*) and number of active cells (*C*) (average of 10 simulations) of the P5–P8 OB-aPC circuits with GABA input (red dots), without GABA input (black dots), and adult GABA input profile (green dots), collected at every 0.5 msec in a 200-msec window of simulation. The simulation (from 0 msec to 53,000 msec) was carried out over several respiratory cycles modulating the activity of the mitral cells, starting with 200 msec of the exhalation phase followed by 200-msec inhalation phase. Activity was measured during the inhalation and exhalation phase. The circuit P5–P8 OB-aPC with GABA input was submitted to seven trials of odor-NE pairing (simulation carried out from 0 msec to 47,000 msec) and 1 sec after the last pairing the GABA synaptic input ($E_{GABA} = -25$ mV) was switched to adult profile ($E_{GABA} = -70$ mV, approximate value based on experimental data reported in Kapur et al. 1997; Whalley and Constanti 2006; Kfir et al. 2020) or blocked (without GABA) (red arrows indicate the beginning of the switch; simulation carried out from 48,000 msec to 53,000 msec). Under those conditions, the mean of cumulative number of spikes and the number of active cells were significant higher in the circuits with GABA input than in the circuits without or with adult profile (inserted graphs). Asterisks represent statistically significant one-way ANOVA comparison among the three condition groups followed by Tukey's multiple comparisons test. (****) $P < 0.0001$. Bin: 0.5 msec.

Neuron model

All neurons were modeled as single compartment leaky integrate-and-fire neurons, in which the change in the membrane voltage is described by Equation 1:

$$\frac{dV(t)}{dt} = \frac{1}{C}\{I_e(t) - g_L[V(t) - E_L]\}, \quad (1)$$

where V (t) is the membrane potential, C is the capacitance, g_L is the leaky membrane conductance, E_L is the resting potential, and I_e is the time-dependent external current input adapted from previous work (Oruro et al. 2020). A particular external input (I_e^{ij}) that a neuron i receives from a presynaptic neuron j at time t is given by Equation 2:

$$I_e^{ij}(t) = W_{ij}g_{ij}(t)[E_{N,ij} - V_i(t)], \quad (2)$$

where W_{ij} is the synaptic strength of the synapse connecting neurons i and j, g_{ij} (t) is the change of channel conductance at time t, $E_{N,ij}$ is the reversal potential of the specific channel type and V_i (t) is the membrane potential of the postsynaptic neuron at time t. The firing probability of the model neuron at voltage V is described by Equation 3:

$$F_i(\mathrm{V}) = \begin{cases} 0 & \text{if } \mathrm{V} < \theta^{\min} \\ \left(\dfrac{\mathrm{V} - \theta^{\min}}{\theta^{\max} - \theta^{\min}}\right)^{\beta} & \text{if } \mathrm{V} \in [\theta^{\min}, \theta^{\max}] \\ 1 & \text{if } \mathrm{V} > \theta^{max} \end{cases}, \quad (3)$$

where θ^{max} represents the saturation value of the threshold, $\theta^{\min}$ is the minimum value of the threshold, and β is a constant defining the nonlinearity of F_i (V). At each spike of the presynaptic neuron j the corresponding conductance in the postsynaptic neuron i changes according to Equation 4:

$$g_{ij}(t) = g_{ij}^{max}\left[exp\left(\frac{-t + t_j^{fire}}{\tau_{1,ij}}\right) - exp\left(\frac{-t + t_j^{fire}}{\tau_{2,ij}}\right)\right], \quad (4)$$

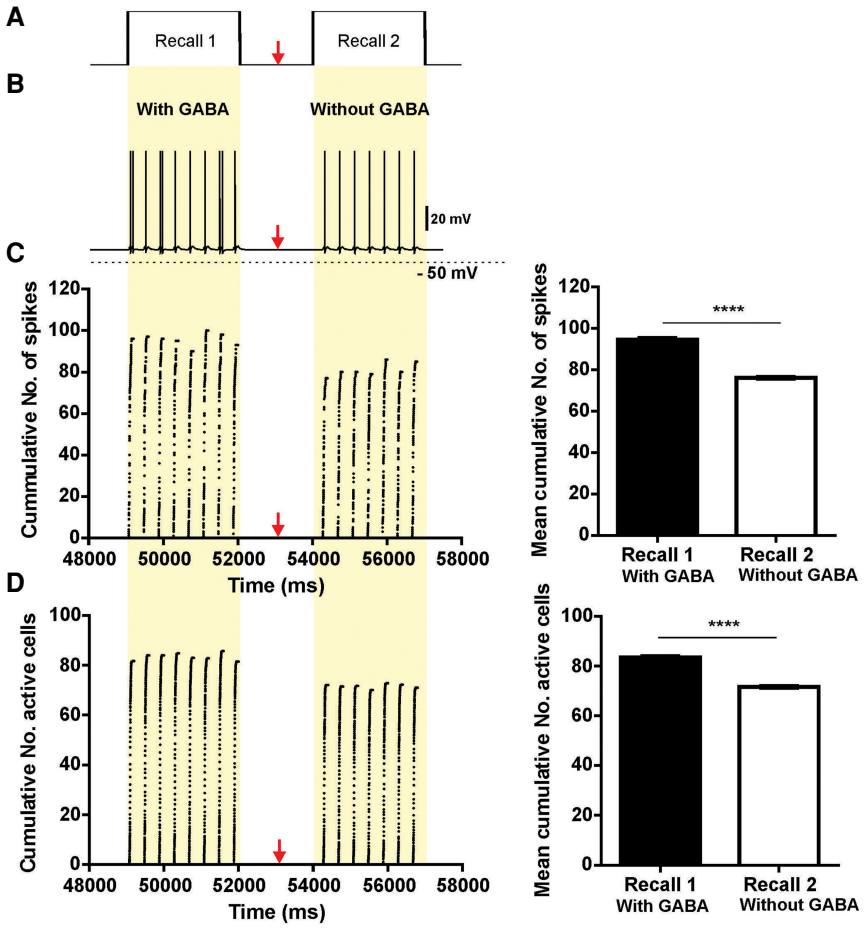

Figure 5. Activity of pyramidal cells during maternal odor recall in the P5–P8 OB-aPC circuit with and without GABA synaptic input. (*A*) Protocol of two periods of maternal odor recall. Two seconds after the last odor-NE pairing (simulation carried out from 0 msec to 47,000 msec), the circuit was exposed to the odor for 3 sec (recall 1) and 2 sec after it has finished, the circuit was exposed again to the odor for 3 sec (recall 2) (simulation carried out from 48,000 msec to 57,000 msec). At the middle of the interval, the circuits have their GABA input profile blocked (red arrows indicate the beginning of the switch, corresponding to 53,000 msec of simulation). The simulation (from 0 msec to 57,000 msec) was carried out over several respiratory cycles modulating the activity of the mitral cells, starting with 200 msec of the exhalation phase followed by 200-msec inhalation phase. Activity was measured during the inhalation and exhalation phase and date were collected at every 0.5 msec in a 200-msec window of simulation. (*B*) Action potential traces of one pyramidal cell during the recall 1 and recall 2. Note that during recall 2 the cell reduced its firing frequency. Plot of cumulative number of spikes (*C*) and number of active cells (*D*) (average of 10 simulations) of the P5–P8 OB-aPC circuits during recall 1 and recall 2. Note that during the recall 2 (circuits without GABA synaptic input) the number of spikes and number of active pyramidal reduced significantly (inserted graphs). Asterisks represent statistically significant unpaired *t* Student test comparison between recall 1 and recall 2. (****) $P<0.0001$. Bin: 0.5 msec.

where t_j^{fire} is the spike time of neuron *j*, g_{ij}^{max} represents the maximum conductance of the corresponding channel, while $\tau_{1,ij}$ and $\tau_{2,ij}$ are its rise and fall. Following an action potential, the voltage of each neuron is reset to the hyperpolarization potential V^{hyper}, where it remains clamped for the refractory period t^{refract}.

In the model, Pyr cells adaptation was implemented as a change in the voltage V_i^{ahc} (t) due to a hyperpolarizing current that increases the firing threshold for the recently activated Pyr neuron *i*, described by Equation 5:

$$\tau^{ahc}\frac{dV_i^{ahc}}{dt}+V_i^{ahc}=A^{ahc}X_i, \tag{5}$$

where X_i is equal to 1 in the time-step after neuron *i* spikes and 0 otherwise. Accordingly, V^{ahc} increases with the constant A^{ahc} and decays with the characteristic time τ^{ahc}.

The output from Mt cells is modulated by a sinusoidal wave of 2 Hz, which mimics the respiratory rhythm (Uchida and Mainen 2003; Kepecs et al. 2007; Verhagen et al. 2007; Wesson et al.

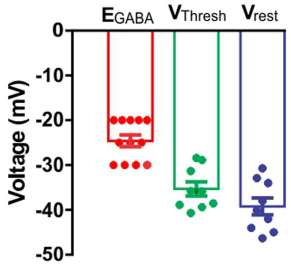

Figure 6. The reversal potential for the $GABA_AR$- mediated synaptic currents in P5–P8 L2/3 aPC pyramidal cells are more depolarized than the V_{rest} and V_{Thresh}. Bar graph showing comparison of mean (±SEM) values of reversal potential for the $GABA_AR$-mediated synaptic currents (E_{GABA}), resting membrane potential (V_{rest}) and the threshold potential (V_{Thresh}). The value for E_{GABA} is more positive than V_{rest} and V_{Thresh}, suggesting that during the P5–P8 age period, the GABAergic synaptic transmission mediated by $GABA_A$ receptors could result in the depolarization of the membrane potentials of the L2/3 aPC pyramidal cells. The bar graph was generated using data described in Table 2.

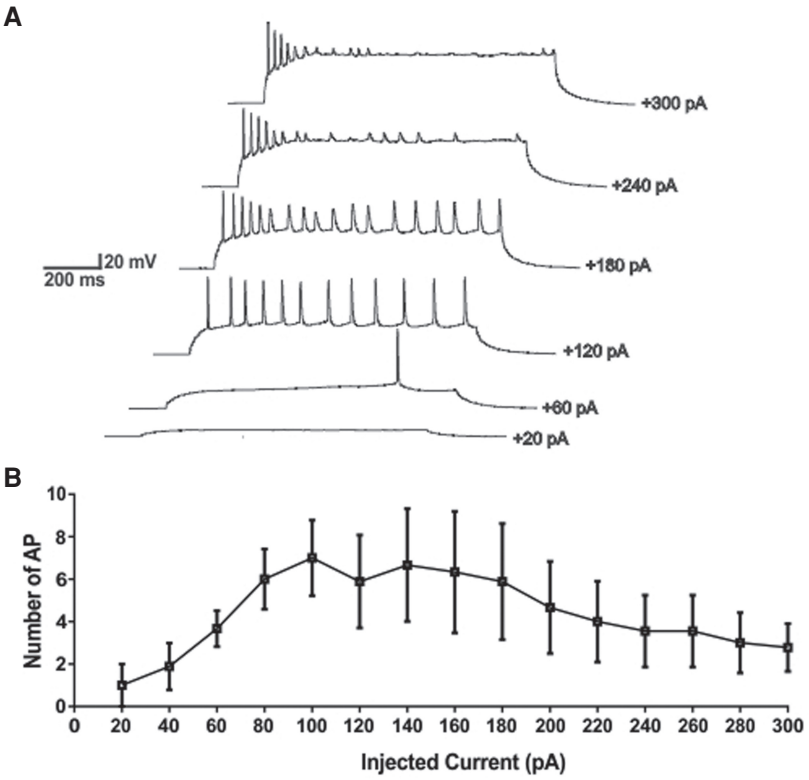

Figure 7. In P5–P8, the firing responses of L2/3 aPC pyramidal cells show adaptive properties to increasing depolarizing currents. Firing properties of the L2/3 aPC pyramidal cells were estimated in the current-clamp mode by applying depolarizing current steps (1 sec of constant current injection). (*A*) Representative traces of pyramidal cell responding to steps of depolarizing currents. Note how the cells reduced its firing at higher intensities of injected currents. (*B*) For depolarizing currents >180 pA, the cells responded by reducing their spike rates. Data are mean (± SEM) values from nine cells. The graphs were generated based in our previous work (Oruro et al. 2020).

2008; Poo and Isaacson 2009). Based on in vivo experimental studies in rodents (Poo and Isaacson 2009; Haddad et al. 2013; Stern et al. 2018) we simulated the activity of mitral cells over the course of several respiratory cycles, with a single respiratory cycle consisting of a 200-msec exhalation followed by a 200-msec inhalation. The onset of odor stimulation was set to coincide with the beginning of the exhalation phase. In the model, only Mt cells received NE modulation.

Synaptic plasticity model

Similar to de Almeida et al. (2013, 2016), activity-dependent synaptic plasticity (Hebbian learning) was implemented for synapses from Mt to Pyr and from Pyr to Pyr. The synaptic strength W_{ij} is increased if both presynaptic and postsynaptic neurons fire together; otherwise, it is reduced to a plasticity rate of 0.25, which multiplies the change of W. This change described by Equation 6:

$$\frac{dW_{ij}}{dt} = (W_{LTP} - W_{ij})\frac{i^{post}\left(t - t_i^{fire}\right)b^{glu}\left(t - t_j^{fire} - t^{delay}\right)}{\tau^{pp}} + (W_{LTD} - W_{ij})\left[\frac{i^{post}\left(t - t_i^{fire}\right)}{\tau^{npp}} + \frac{b^{glu}\left(t - t_j^{fire} - t^{delay}\right)}{\tau^{pnp}}\right], \quad (6)$$

where t^{delay} is the time it takes for the action potential to travel from the soma to the recurrent collateral connections, and i^{post} is the postsynaptic depolarization attributed to retropropagated action potential of postsynaptic neurons described by Equation 7:

$$i^{post}(t) = \frac{t}{\tau^{post}} exp\left(1 - \frac{t}{\tau^{post}}\right), \quad (7)$$

where the time course of the depolarization at the postsynaptic neuron (τ^{post}) is of 2 msec. b^{glu} is the time course of the kinetics of the binding of glutamate on NMDA receptors (de Almeida et al. (2013, 2016) is described by Equation 8.

$$b^{glu}(t) = exp\left(\frac{-t}{\tau^{NMDAf}}\right) \times \left[1 - exp\left(\frac{-t}{\tau^{NMDAr}}\right)\right], \quad (8)$$

where τ^{NMDAf} (7 msec) and τ^{NMDAr} (1 msec) characterize the NMDA receptor kinetics.

During early postnatal weeks, NMDA receptors predominate at the LOT-aPC synapses (Mt-Pyr) (Franks and Isaacson 2005), and these synapses express a robust NMDA-dependent LTP plasticity with strength declining by the first postnatal month. However, the associative synapses (Pyr to Pyr) plasticity do not lose strength in the same period (Poo and Isaacson 2007). The maximum weight for LTP (W_{LTP}) was set initially to 62.2 and the minimal weight for LTD (W_{LTD}) was set initially to 12.25. If i^{post} and i^{post} peak together, then the synaptic weight between the neurons *i* and *j* is driven to (W_{LTP}) with the characteristics time τ^{pp} (12 msec) otherwise, in the case of unsynchronized firing, it is reduced to (W_{LTD})_with the time constant $\tau^{pnp} = \tau^{npp} = 500$ msec.

Experimental data

In our previous work, we reported characteristics of the $GABA_A$ receptor-mediated spontaneous inhibitory postsynaptic currents (sIPSC) obtained by patch-clamp recordings in voltage-clamp mode from pyramidal neurons in layer 2/3 (L2/3) of the aPC in vitro slice preparation of the P5–P8 rat brain slices (Pardo et al. 2018). In some of those recordings from control animals, we identified the $GABA_A$ receptor equilibrium potential (E_{GABA}) by systematically varying the holding potential from 0 to −100 mV in 5-mV-steps. The holding potential where the E_{GABA} has its current zero was considered as a potential for reversion. The analysis of E_{GABA} was carried out by pClamp 10.0 software, through the measurement of the amplitude (pA) of the sIPSC in each step of holding potential tested. Results from this experiment are reported in Table 2.

Acknowledgments

E.M.O. is supported by Coordenação de Aperfeiçoamento de Pessoal de Nível Superior (CAPES; process no. 1608346). G.V.E.P. is supported by a doctoral scholarship from Conselho Nacional de Pesquisa e Desenvolvimento Cientifico e Tecnológico (CNPq; process no. 141727/2014-4). A.B.L. and M.E.C. are funded by CNPq (process no. 465671/2014-4). M.A.P.I. is supported by CNPq (process no. 423843/2016-8). Other funding that partly contributed to the end of this work is provided to G.V.E.P. by Universidad de Ciencias y Humanidades (UCH) under research grant "Exploración teórico-experimental neurocomportamental de la formación del apego madre-infante en el desarrollo temprano" (resolución no. 012-2019-CU-UCH).

Table 2. Experimental data obtained by recording L2/3 aPC pyramidal cells during P5–P8 age

Passive and active membrane properties (mean data)		GABAergic synaptic properties (sIPSC) (mean data)	
V_{res}	−39.22 mV[a]	sIPSC amplitude	11.61 pA[b]
R_{inp}	438.6 MΩ[a]	sIPSC 10%–90% rise time	4.88 msec[b]
Tm	42.78 ms[a]	sPSC Decay-time constant	5.36 msec[b]
Capacitance	98.21 pF[a]	E_{GABA}	−24.58 ± 1.3 mV[c]
AP threshold (mV)	−36.63 mV[a]		
AP amplitude (mV)	76.90 mV[a]		

[a]Data are from Oruro et al. 2020.
[b]Data are from Pardo et al. 2018.
[c]Mean value (±SEM) from 12 pyramidal cells recorded.

References

Al Aïn S, Perry RE, Nuñez B, Kayser K, Hochman C, Brehman E, LaComb M, Wilson DA, Sullivan RM. 2017. Neurobehavioral assessment of maternal odor in developing rat pups: implications for social buffering. *Soc Neurosci* **12:** 32–49. doi:10.1080/17470919.2016.1159605

Bekkers JM, Suzuki N. 2013. Neurons and circuits for odor processing in the piriform cortex. *Trends Neurosci* **36:** 429–438. doi:10.1016/j.tins.2013.04.005

Ben-Ari Y. 2014. The GABA excitatory/inhibitory developmental sequence: a personal journey. *Neuroscience* **279:** 187–219. doi:10.1016/j.neuroscience.2014.08.001

de Almeida L, Idiart M, Linster C. 2013. A model of cholinergic modulation in olfactory bulb and piriform cortex. *J Neurophysiol* **109:** 1360–1377. doi:10.1152/jn.00577.2012

de Almeida L, Idiart M, Dean O, Devore S, Smith DM, Linster C. 2016. Internal cholinergic regulation of learning and recall in a model of olfactory processing. *Front Cell Neurosci* **10:** 256. doi:10.3389/fncel.2016.00256

Ehrlich DE, Ryan SJ, Hazra R, Guo J-D, Rainnie DG. 2013. Postnatal maturation of GABAergic transmission in the rat basolateral amygdala. *J Neurophysiol* **110:** 926–941. doi:10.1152/jn.01105.2012

Farrell WJ, Alberts JR. 2002. Stimulus control of maternal responsiveness to Norway rat (Rattus norvegicus) pup ultrasonic vocalizations. *J Comp Psychol* **116:** 297–307. doi:10.1037/0735-7036.116.3.297

Franks KM, Isaacson JS. 2005. Synapse-specific downregulation of NMDA receptors by early experience: a critical period for plasticity of sensory input to olfactory cortex. *Neuron* **47:** 101–114. doi:10.1016/j.neuron.2005.05.024

Ghosh A, Purchase NC, Chen X, Yuan Q. 2015. Norepinephrine modulates pyramidal cell synaptic properties in the anterior piriform cortex of mice: age-dependent effects of β-adrenoceptors. *Front Cell Neurosci* **9:** 450. doi:10.3389/fncel.2015.00450

Ghosh A, Mukherjee B, Chen X, Yuan Q. 2017. β-Adrenoceptor activation enhances L-type calcium channel currents in anterior piriform cortex pyramidal cells of neonatal mice: implication for odor learning. *Learn Mem* **24:** 132–135. doi:10.1101/lm.044818.116

Haddad R, Lanjuin A, Madisen L, Zeng H, Murthy VN, Uchida N. 2013. Olfactory cortical neurons read out a relative time code in the olfactory bulb. *Nat Neurosci* **16:** 949–957. doi:10.1038/nn.3407

Kapur A, Pearce RA, Lytton WW, Haberly LB. 1997. GABA(A)-mediated IPSCs in piriform cortex have fast and slow components with different properties and locations on pyramidal cells. *J. Neurophysiol* **78:** 2531–2545. doi:10.1152/jn.1997.78.5.2531

Kepecs A, Uchida N, Mainen ZF. 2007. Rapid and precise control of sniffing during olfactory discrimination in rats. *J Neurophysiol* **98:** 205–213. doi:10.1152/jn.00071.2007

Kfir A, Awasthi R, Ghosh S, Kundu S, Paul B, Lamprecht R, Barkai E. 2020. A cellular mechanism of learning-induced enhancement of synaptic inhibition: PKC-dependent upregulation of KCC2 activation. *Sci Rep* **10:** 962. doi:10.1038/s41598-020-57626-2

Kimura F, Nakamura S. 1985. Locus coeruleus neurons in the neonatal rat: electrical activity and responses to sensory stimulation. *Brain Res* **355:** 301–305. doi:10.1016/0165-3806(85)90055-0

Kojima S, Alberts JR. 2009. Maternal care can rapidly induce an odor-guided huddling preference in rat pups. *Dev Psychobiol* **51:** 95–105. doi:10.1002/dev.20349

Meyer PM, Alberts JR. 2016. Non-nutritive, thermotactile cues induce odor preference in infant mice (Mus musculus). *J Comp Psychol* **130:** 369–379. doi:10.1037/com0000044

Moriceau S, Sullivan RM. 2004. Unique neural circuitry for neonatal olfactory learning. *J Neurosci* **24:** 1182–1189. doi:10.1523/JNEUROSCI.4578-03.2004

Moriceau S, Sullivan RM. 2005. Neurobiology of infant attachment. *Dev Psychobiol* **47:** 230–242. doi:10.1002/dev.20093

Morrison GL, Fontaine CJ, Harley CW, Yuan Q. 2013. A role for the anterior piriform cortex in early odor preference learning: evidence for multiple olfactory learning structures in the rat pup. *J Neurophysiol* **110:** 141–152. doi:10.1152/jn.00072.2013

Mukherjee B, Yuan Q. 2016. NMDA receptors in mouse anterior piriform cortex initialize early odor preference learning and L-type calcium channels engage for long-term memory. *Sci Rep* **6:** 35256. doi:10.1038/srep35256

Okutani F, Zhang JJ, Otsuka T, Yagi F, Kaba H. 2003. Modulation of olfactory learning in young rats through intrabulbar GABAB receptors. *Eur J Neurosci* **18:** 2031–2036. doi:10.1046/j.1460-9568.2003.02894.x

Oruro EM, Pardo GVE, Lucion AB, Calcagnotto ME, Idiart MAP. 2020. Maturation of pyramidal cells in anterior piriform cortex may be sufficient to explain the end of early olfactory learning in rats. *Learn Mem* **27:** 20–32. doi:10.1101/lm.050724.119

Pardo GVE, Lucion AB, Calcagnotto ME. 2018. Postnatal development of inhibitory synaptic transmission in the anterior piriform cortex. *Int J Dev Neurosci* **71:** 1–9. doi:10.1016/j.ijdevneu.2018.07.008

Perry RE, Blair C, Sullivan RM. 2017. Neurobiology of infant attachment: attachment despite adversity and parental programming of emotionality. *Curr Opin Psychol* **17:** 1–6. doi:10.1016/j.copsyc.2017.04.022

Poo C, Isaacson JS. 2007. An early critical period for long-term plasticity and structural modification of sensory synapses in olfactory cortex. *J Neurosci* **27:** 7553–7558. doi:10.1523/JNEUROSCI.1786-07.2007

Poo C, Isaacson JS. 2009. Odor representations in olfactory cortex: 'sparse' coding, global inhibition, and oscillations. *Neuron* **62:** 850–861. doi:10.1016/j.neuron.2009.05.022

Raineki C, Moriceau S, Sullivan RM. 2010. Developing a neurobehavioral animal model of infant attachment to an abusive caregiver. *Biol Psychiatry* **67:** 1137–1145. doi:10.1016/j.biopsych.2009.12.019

Rangel S, Leon M. 1995. Early odor preference training increases olfactory bulb norepinephrine. *Brain Res Dev Brain Res* **85:** 187–191. doi:10.1016/0165-3806(94)00211-H

Rheims S, Minlebaev M, Ivanov A, Represa A, Khazipov R, Holmes GL, Ben-Ari Y, Zilberter Y. 2008. Excitatory GABA in rodent developing neocortex in vitro. *J Neurophysiol* **100:** 609–619. doi:10.1152/jn.90402.2008

Rivera C, Voipio J, Payne JA, Ruusuvuori E, Lahtinen H, Lamsa K, Pirvola U, Saarma M, Kaila K. 1999. The K+/Cl– co-transporter KCC2 renders GABA hyperpolarizing during neuronal maturation. *Nature* **397:** 251–255. doi:10.1038/16697

Ross JM, Fletcher ML. 2019. Aversive learning-induced plasticity throughout the adult mammalian olfactory system: insights across development. *J Bioenerg Biomembr* **51:** 15–57. doi:10.1007/s10863-018-9770-z

Roth TL, Raineki C, Salstein L, Perry R, Sullivan-Wilson TA, Sloan A, Lalji B, Hammock E, Wilson DA, Levitt P, et al. 2013. Neurobiology of secure infant attachment and attachment despite adversity: a mouse model. *Genes Brain Behav* **12:** 673–680. doi:10.1111/gbb.12067

Stern M, Bolding KA, Abbott L, Franks KM. 2018. A transformation from temporal to ensemble coding in a model of piriform cortex. *Elife* **7:** e34831. doi:10.7554/elife.34831

Stokes CCA, Isaacson JS. 2010. From dendrite to soma: dynamic routing of inhibition by complementary interneuron microcircuits in olfactory cortex. *Neuron* **67:** 452–465. doi:10.1016/j.neuron.2010.06.029

Sullivan RM, Opendak M. 2018. Developmental and neurobehavioral transitions in survival circuits. *Curr Opin Behav Sci* **24:** 50–55. doi:10.1016/j.cobeha.2018.03.005

Sullivan RM, McGaugh JL, Leon M. 1991. Norepinephrine-induced plasticity and one-trial olfactory learning in neonatal rats. *Brain Res Dev Brain Res* **60:** 219–228. doi:10.1016/0165-3806(91)90050-S

Sullivan RM, Zyzak DR, Skierkowski P, Wilson DA. 1992. The role of olfactory bulb norepinephrine in early olfactory learning. *Brain Res Dev Brain Res* **70:** 279–282. doi:10.1016/0165-3806(92)90207-D

Sullivan RM, Wilson DA, Lemon C, Gerhardt GA. 1994. Bilateral 6-OHDA lesions of the locus coeruleus impair associative olfactory learning in newborn rats. *Brain Res* **643:** 306–309. doi:10.1016/0006-8993(94)90038-8

Sullivan RM, Stackenwalt G, Nasr F, Lemon C, Wilson DA. 2000. Association of an odor with activation of olfactory bulb noradrenergic β-receptors or locus coeruleus stimulation is sufficient to produce learned approach responses to that odor in neonatal rats. *Behav Neurosci* **114:** 957–962. doi:10.1037/0735-7044.114.5.957

Suzuki N, Bekkers JM. 2007. Inhibitory interneurons in the piriform cortex. *Clin Exp Pharmacol Physiol* **34:** 1064–1069. doi:10.1111/j.1440-1681.2007.04723.x

Thompson JV, Sullivan RM, Wilson DA. 2008. Developmental emergence of fear learning corresponds with changes in amygdala synaptic plasticity. *Brain Res* **1200:** 58–65. doi:10.1016/j.brainres.2008.01.057

Tyzio R, Nardou R, Ferrari DC, Tsintsadze T, Shahrokhi A, Eftekhari S, Khalilov I, Tsintsadze V, Brouchoud C, Chazal G, et al. 2014. Oxytocin-mediated GABA inhibition during delivery attenuates autism pathogenesis in rodent offspring. *Science* **343:** 675–679. doi:10.1126/science.1247190

Uchida N, Mainen ZF. 2003. Speed and accuracy of olfactory discrimination in the rat. *Nat Neurosci* **6:** 1224–1229. doi:10.1038/nn1142

Verhagen JV, Wesson DW, Netoff TI, White JA, Wachowiak M. 2007. Sniffing controls an adaptive filter of sensory input to the olfactory bulb. *Nat Neurosci* **10:** 631–639. doi:10.1038/nn1892

Wesson DW, Donahou TN, Johnson MO, Wachowiak M. 2008. Sniffing behavior of mice during performance in odor-guided tasks. *Chem Senses* **33:** 581–596. doi:10.1093/chemse/bjn029

Whalley BJ, Constanti A. 2006. Developmental changes in presynaptic muscarinic modulation of excitatory and inhibitory neurotransmission in rat piriform cortex in vitro: relevance to epileptiform bursting susceptibility. *Neuroscience* **140:** 939–956. doi:10.1016/j.neuroscience.2006.02.046

Wilson DA, Sullivan RM. 1992. Blockade of mitral/tufted cell habituation to odors by association with reward: a preliminary note. *Brain Res* **594:** 143–145. doi:10.1016/0006-8993(92)91039-H

Yuan Q, Shakhawat AMD, Harley CW. 2014. Mechanisms underlying early odor preference learning in rats. *Prog Brain Res* **208:** 115–156. doi:10.1016/B978-0-444-63350-7.00005-X

Received June 21, 2020; accepted in revised form September 27, 2020.